Physica C 512 (2015) 32–41

Contents lists available at ScienceDirect

Physica C

journal homepage: www.elsevier.com/locate/physc

Critical current and flux pinning properties of the superconducting Ti–V alloys

Md. Matin [a], L.S. Sharath Chandra [a], M.K. Chattopadhyay [a,*], R.K. Meena [a], Rakesh Kaul [b], M.N. Singh [c], A.K. Sinha [c], S.B. Roy [a]

[a] Magnetic & Superconducting Materials Section, Raja Ramanna Centre for Advanced Technology, Indore 452 013, India
[b] Laser Material Processing Division, Raja Ramanna Centre for Advanced Technology, Indore 452 013, India
[c] Indus Synchrotrons Utilization Division, Raja Ramanna Centre for Advanced Technology, Indore 452 013, India

ARTICLE INFO

Article history:
Received 23 January 2015
Accepted 26 February 2015
Available online 6 March 2015

Keywords:
Flux pinning
Critical current
Dislocation

ABSTRACT

We present a study on the critical current density and the flux-line pinning properties of a series of annealed and as cast samples of $Ti_{100-x}V_x$ (x = 20, 30, 40 and 60) alloys, performed with the help of magnetization measurements. We show that the grain boundaries are the dominant flux pinning centers in the Ti–V alloys in the low and intermediate magnetic field regime. In the high magnetic field regime, the dislocation networks and the point pinning mechanism provided by the ω phase present in these alloys are more effective than the grain boundaries. While in the low magnetic fields we find the signature of surface effects enhancing the pinning force density, a peak effect in the critical current is observed in these alloys in the high field regime near the upper critical field H_{C2}. Using the existing theories we provide an analysis of the pinning force density over a large range of magnetic fields, and obtain some new insight on the influence of various metallurgical phases, grain boundaries and dislocation networks on the flux-line pinning properties of these alloys.

1. Introduction

The Ti–V superconductors are currently drawing attention because of their suitability for applications in the environments where the superconducting components may be subjected to long term irradiation, and their high degree of machinability [1]. Their technological applications will, however, depend on the optimization of the relevant superconducting properties like the critical current density (J_C), which depends crucially on the structural and metallurgical aspects of the material. The well-established metallurgical phase diagram of the Ti–V alloy system [2] gives an idea of structural and metallurgical properties of this system. The magnetic field dependence of critical current density J_C of the Ti–V alloys is not thoroughly studied [1], and thus there is scope to investigate the effects of various kinds of structural defects [3] and impurity phases on the flux pinning properties of these alloys. This in turn may provide clues for tuning the superconducting properties for future applications. In the present work we study the critical current density and flux-line pinning force density in a series of annealed and as cast samples of Ti–V alloys covering mostly the Ti-rich region of the metallurgical phase diagram.

The metallurgical features of the Ti–V alloy system varies considerably across the phase diagram. To highlight this we present in Fig. 1 the phase diagram of the Ti–V alloy system derived from the literature [2] along with the superconducting transition temperature (T_C) corresponding to the present alloys. In the present work, we focus on the composition regime with 20% to 60% V. In this composition regime the T_C of the Ti–V alloys reach a plateau around 40% V (see Fig. 1). In a recent study we have shown the correlation between the J_C and the flux pinning force density (F_P) (for a limited range of applied magnetic field) with the metallurgical phases and the associated defect structures in the as cast and annealed samples of the $Ti_{60}V_{40}$ and $Ti_{70}V_{30}$ alloys [4]. We inferred that while the grain boundaries and dislocation arrays act as the major normal surface pins for the flux-lines in these alloys, the hexagonal ω phase present in the system functions as normal point pins. On the other hand, our study also indicated that the boundaries of the columnar grains can form a percolation network that can act as flux flow channels in this system [4]. Since the flux pinning properties of the Ti–V alloys are influenced by different kinds of lattice defects, it is important to find out the relative effectiveness of these defects in different magnetic field regimes.

* Corresponding author.
E-mail address: maulindu@rrcat.gov.in (M.K. Chattopadhyay).

http://dx.doi.org/10.1016/j.physc.2015.02.049
0921-4534/

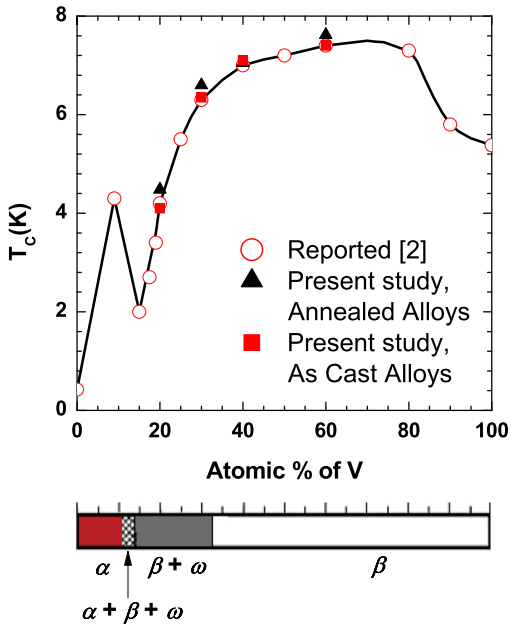

Fig. 1. Composition dependence of the superconducting transition temperature and the structural properties of the Ti–V alloys.

In order to obtain deeper understanding on these aspects, we now present a study of critical current density J_C and pinning force density F_P in the Ti–V alloys over a wider compositional range and also a wider magnetic field regime. In this direction we have (i) prepared two newer compositions of Ti–V alloys namely $Ti_{80}V_{20}$ and $Ti_{40}V_{60}$ and have studied them through X-ray diffraction (XRD), optical metallography, and dc magnetization measurements; (ii) analyzed the field dependence of pinning force density in these four different Ti–V alloys (both in the as-cast and annealed conditions) in all field regimes starting from zero to the limit of the upper critical field and identified the different pinning mechanisms prevalent in different field regimes; and (iii) investigated the influence of the metallurgical phases, material defects, surface barrier effects, and the shear strength of the flux-line lattice on the pinning mechanisms effective in different magnetic field regimes.

2. Experimental details

Polycrystalline samples of as cast and annealed $Ti_{80}V_{20}$, $Ti_{70}V_{30}$, $Ti_{60}V_{40}$ and $Ti_{40}V_{60}$ alloys have been used for the present study. High purity Ti (99.99 %, Alfa Aesar) and V (99+%, Aldrich) were taken in atomic proportions, and were melted in an arc-melting furnace under high purity (99.99+%) Ar atmosphere to form the as cast alloys. Metallic Ti was used as the getter material during this melting process, and the ingots were flipped and re-melted four times to ensure the homogeneity. Portions of the as cast ingots were then wrapped in Ta-foil and sealed in quartz ampoules in argon atmosphere and annealed at 1300 °C for 10 h. The sample temperature was then lowered to 1000 °C before quenching into ice-water. The structural characterization of both the annealed and as cast samples was done through angle dispersive X-ray diffraction (XRD) measurements performed in a powder XRD beam line (BL-12) [5] at 19 keV energy (0.65×10^{-10} m) using the X-rays from INDUS-2 synchrotron radiation source in the Raja Ramanna Centre for Advanced Technology, Indore. The beam line is based on Si (3 1 1) double crystal monochromator and adaptive focusing optics. An image plate area detector (MAR-345 dtb) and Fit2d software were used for data acquisition and data reduction, respectively. NIST LaB_6 standard was used for wavelength calibration. The optical metallography of the samples was done using a high power optical microscope (Olympus, PME-3). Before doing these optical metallography experiments, the samples were polished using fine diamond paste and etched chemically using a dilute solution of HF and HNO_3 dissolved in distilled water. The magnetization (M) measurements were done as a function of temperature (T, 2–8 K) and magnetic field (B, up to 8 T) using a Vibrating Sample Magnetometer (VSM; Quantum Design, USA).

3. Results and discussion

3.1. Structural and metallographic characterization

Fig. 2 shows the XRD patterns for the annealed and as cast samples of the $Ti_{80}V_{20}$ and $Ti_{40}V_{60}$ alloys. The XRD patterns of the other sample used in the present study have already been reported earlier [4]. The XRD patterns were analyzed using the Rietveld refinement technique (the individual fitted curves are not shown here for the sake of clarity and conciseness). The analysis of the XRD patterns indicate the presence of four metallurgical phases: The main β phase with a body centered cubic (bcc) structure (space group: $Im\bar{3}m$), the ω phase with a hexagonal $P6/mmm$ symmetry, the α phase with a hexagonal $P63/mmc$ symmetry, and a stress induced orthorhombic phase α' (space group: $Cmcm$). The lattice parameters and relative phase fractions obtained from the analysis of the XRD patterns for all the alloys used in the present work (the as cast and annealed $Ti_{80}V_{20}$, $Ti_{70}V_{30}$, $Ti_{60}V_{40}$ and $Ti_{40}V_{60}$ alloys) are summarized in Table 1, though only the indices for the major peaks corresponding to the main β phase of the annealed and as cast samples of the $Ti_{80}V_{20}$ and $Ti_{40}V_{60}$ alloys are indexed in Fig. 2 (for clarity). The presence of α and ω phases along with the β phase in the Ti–V alloys has been reported previously, and the lattice parameters presented in Table 1 are in agreement with the published literature [2,6]. The stress induced α' phase has also been reported in literature, and is said to form through an athermal transition in some compositions of the Ti–V alloys [7,8].

Fig. 3 shows selected optical micrographs for the as cast and annealed samples of the present Ti–V alloys. The grain size in these

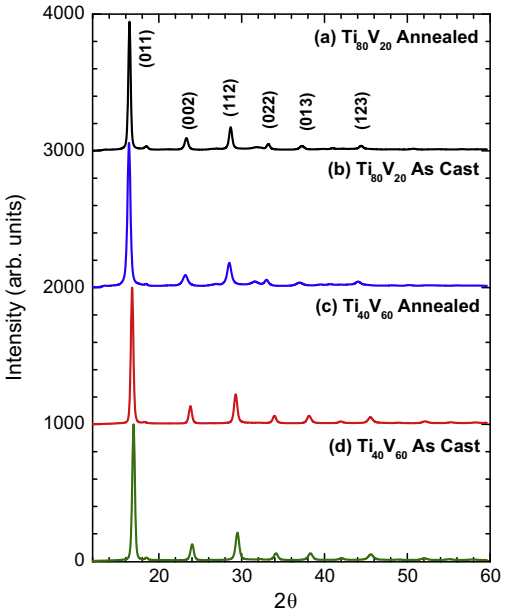

Fig. 2. The XRD patterns of the annealed and as cast samples of the $Ti_{80}V_{20}$ and $Ti_{40}V_{60}$ alloys. Only the indices corresponding to the major peaks in the main phase [body centered cubic (bcc) β phase structure] are shown here.